

Testing CPS with Design Assumptions-Based Metamorphic Relations and Genetic Programming

Claudio Mandrioli, Seung Yeob Shin, *IEEE*, Domenico Bianculli *IEEE*, Lionel Briand *Fellow, IEEE*



Abstract—Cyber-Physical Systems (CPSs) software is used to enforce desired behaviours on physical systems. To test the interaction between the CPS software and the system’s physics, engineers provide traces of desired physical states and observe traces of the actual physical states. CPS requirements describe how closely the actual physical traces should track the desired traces. These requirements are typically defined for specific, simple input traces such as step or ramp sequences, and thus are not applicable to arbitrary inputs. This limits the availability of oracles for CPSs. Our recent work proposes an approach to testing CPS using control-theoretical design assumptions instead of requirements. This approach circumvents the oracle problem by leveraging the control-theoretical guarantees that are provided when the design assumptions are satisfied. To address the test case generation and oracle problems, researchers have proposed metamorphic testing, which is based on the study of relations across tests, i.e., metamorphic relations (MRs). In this work, we define MRs based on the design assumptions and explore combinations of these MRs using genetic programming to generate CPS test cases. This enables the generation of CPS input traces with potentially arbitrary shapes, together with associated expected output traces. We use the deviation from the expected output traces to guide the generation of input traces that falsify the MRs. Our experiment results show that the MR-falsification provides engineers with new information, helping them identify passed and failed test cases. Furthermore, we show that the generation of traces that falsify the MRs is a non-trivial problem, which is successfully addressed by our genetic search.

1 INTRODUCTION

Cyber-Physical Systems (CPSs) are pervasive in modern life. Such systems are characterised by the closed-loop interaction between software and physical parts [1]. The goal of this interaction is to have the software enforce a desired behaviour on the physical part. More precisely, the software should steer the physical part to desired states, for example flying a drone to the desired position. Accordingly, CPS requirements specify the desired behaviour of the physical part rather than the software behaviour. This makes the testing of CPS software a multidisciplinary problem (including aspects of software and control engineering), regarding

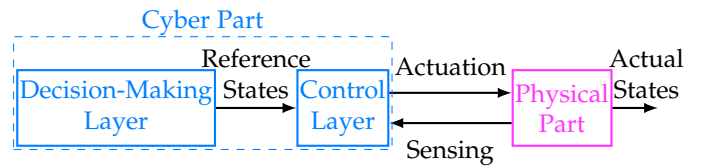


Fig. 1: This figure shows the CPS structure highlighting the role of the control layer in the interaction with the physics. The cyber part is represented by the dashed azure box, and it consists of the decision-making and control layers. The physical part is represented by the purple box. The arrows denote input or output signals.

both the generation of test inputs and the implementation of oracles [2].

Figure 1 shows the structure of a CPS with the cyber part in the dashed azure box, and the physical part in purple. Within the cyber part, the control layer is responsible for the real-time interaction with the physical part, performed through actuators and sensors. Then, the CPS decision-making layer defines a desired physical state (called *reference* in control-engineering jargon) that the control layer should achieve. The control layer, developed collaboratively by software and control engineers, uses sensors and actuators to steer the physical part to the desired state. For example, in a patrolling drone, the decision-making layer decides which areas to target and the path to follow. Then, it sends the sequence of desired positions to the control layer, which is responsible for actually flying the drone through them by identifying the drone position through sensors and sending appropriate commands to actuators.

When testing the software implementing the CPS control layer, engineers define input traces of physical states reference values and observe output traces of the actual states. Intuitively, the requirements define how closely the actual physical state should follow the reference one *depending on a given input shape*. Examples of typical requirements are the steady-state error that prescribes the maximum allowed difference between the desired and actual state when the input is constant, and the overshoot that defines the maximum state value allowed after a step change in the reference (i.e., an instant change followed by constant values) [3]. Such

- C. Mandrioli is with the University of Luxembourg, Luxembourg.
- S. Y. Shin is with the University of Luxembourg, Luxembourg.
- D. Bianculli is with the University of Luxembourg, Luxembourg.
- L. Briand is with the University of Ottawa, Canada, and the University of Limerick, Ireland.

requirements can then be used to assess the CPS for constant inputs and step changes. This tight connection between requirements and a given input trace, in practice, limits the possibility of defining oracles applicable to different traces. Indeed, a CPS is expected to track a variety of input traces, and possibly arbitrary ones. Thus, most of the possible input traces are different from the ones for which the requirements are defined, and it is impossible to define oracles.

Currently, to overcome this limitation, engineers can use the distance between the desired and actual states, i.e., the *control error*, to assess the CPS ability to track the reference states. However, the control error is a coarse metric, and it does not capture properties related to the shape of the input and output traces. Thus, it has limited use as an oracle.

As an alternative to testing CPS based on requirements, in our previous work [2] we proposed a new approach based on control theoretical guarantees. The idea of the approach is to focus on testing scenarios that falsify the *design assumptions* that underlie the CPS mathematical models used by control engineers. In fact, using such mathematical models of the CPS behaviour, control engineers can provide a priori guarantees on the performance of the implemented CPS. Then, when the design assumptions hold in the CPS implementation, we can rely on these guarantees from the control theoretical models for satisfying requirements. In contrast, when the assumptions are falsified, the CPS behaviour is not predicted by the models and therefore it requires empirical verification, i.e., testing. Thus, by testing the design assumptions, we can indirectly obtain guarantees on the requirements satisfaction through the control theoretical guarantees. In our previous work, we focused on how to generate test cases to falsify the *linear behaviour* design assumption [3, 4], which is widely used in CPS development [3, 5, 6]. However, our previous work was limited as it targets the testing of individual CPS states (e.g., only the altitude control in a drone) and requires user-defined periodic input shapes.

When testing CPS, causing failures is not always difficult. Analogously, the sole falsification of the linearity design assumption is not necessarily a difficult task. Specifically, large and fast-changing inputs are likely to falsify the linearity assumption, as they can lead the CPS to an unexpected physical state [2]. Such scenarios correspond to a high degree of falsification of the design assumptions, and can be considered *trivial failures*, as the CPS was never expected to perform such manoeuvres. The more interesting and challenging problem is the generation and identification of *subtle failures*, where a CPS shows subtle behaviour deviations [7, 8]. An example of a subtle deviation is an unexpected oscillation of a patrolling drone, which possibly does not significantly change the control error but can affect the drone’s ability to take pictures of its target. Accordingly, while generating scenarios that falsify the design assumptions, we want at the same time to avoid trivial failures.

Software engineering researchers have proposed Metamorphic Testing (MT) to address both the test case generation and oracle problems [9]. MT is based on Metamorphic Relations (MRs), which are properties defined over multiple inputs and outputs of two or more test cases. Being defined over multiple test cases, the MRs are used in MT to generate new follow-up test cases from initial ones, together with an

associated expected output. In practice, the applicability of MT is limited by the availability of MRs that often have to be defined manually [10], and the automated generation of MRs is still an open problem in general [11, 12]. For example, in recent works that have applied MT to different CPSs, such as cars [13, 14] and UAVs [15], the MRs are defined manually and are specific to the given application scenario.

In this work, we propose to use the design assumptions to define MRs that are valid for any CPS developed with the use of control theory, and apply MT. Specifically, we define MRs based on the control-theoretical design assumption of linear behaviour [4], which are valid across different CPS domains (e.g., drones and automotive systems). Hence, we aim to test the control layer implementation assuming it should behave linearly. We express the linearity properties as MRs between input-output pairs of initial and follow-up tests. Using the MRs, we generate input traces together with their associated expected output traces. Comparing the expected output trace with the actual one, we provide engineers with a new metric, the *MR-falsification degree*, which can be used to identify test cases within the design scope (i.e., those that follow their reference thanks to the control theoretical guarantees) from test cases that are out of the design scope and show unexpected behaviour. Using a Genetic Programming (GP) algorithm, we then combine MR-falsification and control error to guide the generation of input traces and their expected output traces, leading the CPS out of its design scope (i.e., falsify the MRs) while avoiding trivial failures.

Our experiment results show that the problem of falsifying the MRs, while avoiding trivial failures, cannot be addressed with a baseline random approach. The proposed GP approach, however, can generate arbitrary input traces that falsify the MRs and thus the associated design assumptions. Furthermore, our results show that the MR-falsification degree is not correlated with the control error, and thus effectively provides new information for the assessment of CPS test outputs.

To summarise, this article provides the following contributions to the CPS test input generation and oracle problems:

- the definition of MRs based on the linear behaviour design assumption, that are valid independently of the CPS application domain;
- the use of such MRs, in combination with GP and MT, to generate CPS input traces with arbitrary shapes and associated expected output traces, that lead to the falsification of the linearity design assumption, while avoiding trivial failures;
- the extension of our previous work on linearity design assumptions testing to multi-dimensional and non-periodic input traces, with potentially arbitrary shapes;
- the evaluation of the proposed approach on two CPSs from the automotive and drone domains.

The remainder of the article is structured as follows. In Section 2 we present a motivating example of the addressed challenges. In Section 3 we introduce our MRs. In Section 4 we describe the proposed GP approach. In Section 5 we empirically assess our approach. Finally, Sections 6 and 7 conclude the article with the related work and the conclusions.

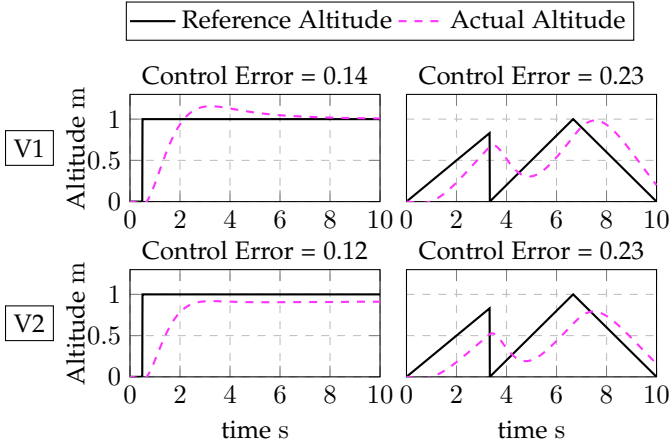


Fig. 2: Examples of step responses of the altitude control of a drone, with the reference input altitude in black and the actual altitude in purple. The left-hand side plots show a step response, where the steady-state error and overshoot are well defined. The right-hand side plots show instead an arbitrary input trace, for which the steady state and overshoot cannot be assessed.

2 MOTIVATING EXAMPLE

In this section, we use the altitude control of a drone to exemplify the challenges addressed in this work. Specifically, we showcase the limitations of requirements defined based on simple input shapes, and the limitations of the control error as an oracle. We conclude the section by defining our testing objective.

Figure 2 shows two flight tests for two different implementations of a drone altitude control, with implementation V1 in the first row and V2 in the second row. In the left-hand side plots, we show the test of a step input trace and, in the right-hand side, an arbitrary trace. In each plot, the solid line represents the reference altitude (i.e., the input trace), and the purple dashed line shows the drone actual altitude (i.e., the test output); thus, the objective is that the actual altitude tracks the reference one.

In the step-input tests, we can directly assess the satisfaction of some requirements, such as the steady-state error and the overshoot. In V1, we observe that the drone eventually reaches precisely the desired altitude when the input is constant, thus showing a zero steady-state error. In contrast, V2 does not reach the desired value, and is thus not satisfying the requirement. The overshoot can be clearly measured at $t = 3$ for V1, when the actual altitude reaches the maximum value. Instead, for V2, the actual output never takes values larger than the desired one, so the overshoot is zero. Thus, for the step input, we can directly check the steady-state error and overshoot requirements. However, for the arbitrary input traces in the right-hand side plots, this assessment is not feasible. First, the input is never constant, preventing the assessment of the steady-state error. In addition, there is no clear time instant at which the overshoot should be assessed, since the input changes linearly rather than in steps. As a result, such requirements are not well-defined for this arbitrary input trace, and oracles for assessing them cannot be implemented.

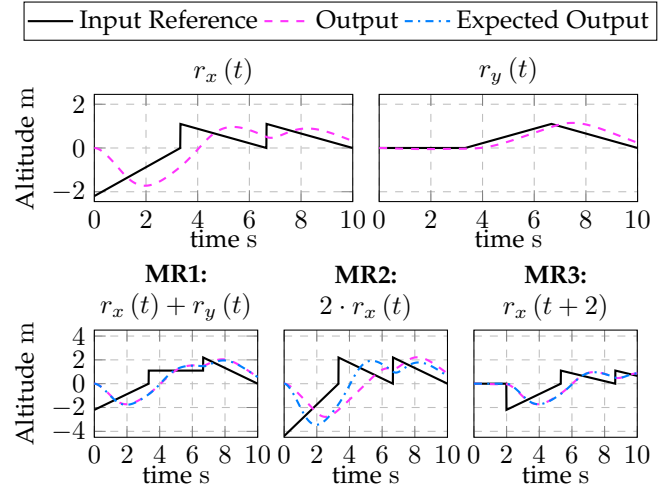


Fig. 3: Example of MRs applications for a simplified drone altitude control example. Starting from the two initial tests in the first row (r_x and r_y) we build three follow-up tests in the bottom row, showcasing MR1, MR2, and MR3, respectively. For the initial tests, we have only the input (black continuous line) and output (purple dashed line) traces. Thanks to the MRs, for the follow up test cases we can also compute the expected output (dash-dotted lines) traces.

When using the control error to assess the tests in Figure 2, we observe that they show very similar values (indicated above the plots, and measured as the average difference between the desired and actual altitudes) for the two versions of the CPS. Specifically, for the arbitrary input, we observe the very same control error value (0.23), and for the step input, we cannot explain the 0.02 difference in control error between V1 and V2 by a different degree of satisfaction of the steady-state error and overshoot requirements. Therefore, the control error, despite being the most intuitive metric for assessing a CPS ability to track references, is not sufficient to implement oracles.

To address the limitations of direct requirements assessment and of control error as CPS oracles, we propose the use of design assumptions. Most importantly, the design assumptions that underlie control theoretical models are independent of the specific input. Further, as mentioned in Section 1, besides the falsification of the design assumptions, we also want to avoid trivial failures. For example, if a drone flies upside-down, the physics models used for the control design lose validity, causing the drone to crash.

Accordingly, we formulate our **testing objective** as the generation of arbitrary input traces, along with their expected output traces, that *falsify the linearity design assumption while avoiding trivial failures*, where we identify trivial failures as test cases with large control errors.

3 METAMORPHIC RELATIONS

Before delving into our approach, we introduce the MRs it relies upon. As mentioned in Section 1, we define the MRs based on the definition of linear time-invariant (LTI) systems [3]. A system G is said to be LTI when it satisfies the three properties below for every input r . In the properties definitions, $r_x(t)$ and $r_y(t)$ are input sequences functions

of time t ; $G[r(t)](t)$, also function of time t , is the system output in response to the input $r(t)$; α and δ are real-valued constants.

PR1: The output generated by the sum of two inputs, is equal to the sum of the outputs generated by the two inputs alone. Mathematically:

$$G[r_x(t) + r_y(t)](t) = G[r_x(t)](t) + G[r_y(t)](t).$$

PR2: The output generated by an input scaled by a constant value, is equal to the output generated by the non-scaled input scaled by the same constant. Mathematically:

$$G[\alpha \cdot r_x(t)](t) = \alpha \cdot G[r_x(t)](t).$$

PR3: The output generated by an input shifted in time, is the same as the output generated by the non-shifted input shifted in time by the same constant. Mathematically:

$$G[r_x(t)](t + \delta) = G[r_x(t + \delta)](t).$$

These properties describe how the output of an LTI system is expected to change when applying specific change patterns to its inputs. In the software testing literature, properties defined over sets of inputs and corresponding System-Under-Test (SUT) outputs are called MRs [10]. Based on the three defining properties of an LTI system, we derive three MRs. Our MRs are logical implications with an *antecedent* that describes the input change pattern and a *consequent* that describes how the output is expected to change.

MR1: If an input is the sum of two other inputs, then its output is the sum of the two initial outputs:

$$r(t) = r_x(t) + r_y(t) \Rightarrow$$

$$G[r(t)](t) = G[r_x(t)](t) + G[r_y(t)](t).$$

MR2: If an input is equal to another input scaled by a factor α , then its output is the same as the initial output scaled by the same factor:

$$r(t) = \alpha \cdot r_x(t) \Rightarrow G[r(t)](t) = \alpha \cdot G[r_x(t)].$$

MR3: If an input is equal to another input shifted in time by a step δ , then its output is the same as the initial output shifted in time by the same quantity:

$$r(t) = r_x(t + \delta) \Rightarrow G[r(t)](t) = G[r_x(t)](t + \delta).$$

The three MRs define equalities between input traces in the antecedent and output traces in the consequent. The equality between input traces (i.e., the antecedent) can be leveraged to construct follow-up input traces. Then, we can run the tests, obtain the tests outputs, and use the consequent to assess whether the MR holds or not, thus effectively serving as oracle. Specifically, we use the output of the initial test cases to obtain the *expected output* $e(t)$ of the follow-up test case, i.e., the expected output trace. Then, if the expected output is equal to the *actual output*, we consider the MR satisfied.

We showcase such use of the MRs in Figure 3, where we run tests on a simplified model of a drone's altitude control.¹

1. The model is simplified in that it only simulates the vertical movement of the drone.

However, we underline that the MRs equally apply in the multi-dimensional case, e.g., if we were to consider all three dimensions x,y,z in which the drone can move. In the figure, we use the two initial test cases reported in the upper plots, r_x and r_y , to construct three follow-up test cases in the lower plots. Each follow-up test case is obtained applying one of the MRs. For the initial test cases we depict the input traces (i.e., the reference) as solid black lines and the output traces obtained after executing them as purple dashed lines. For the follow-up plots, we also depict the expected output traces, built using the consequent of the MRs, with dash-dotted blue lines. For MR1, we obtain a new input trace by summing (superimposing) the two initial input traces, reported in the left-hand side bottom plot. The expected output trace is also obtained by summing the outputs traces of the initial test cases. Since the actual output matches the expected one, we conclude that MR1 is satisfied. In contrast, in the centre bottom plot, we apply MR2 and multiply the input and output traces by 2. In this case, we observe that the actual and expected output do not match, thus *falsifying* the MR. In the right-hand side bottom plot, we apply MR3 and shift in time the test case. We thus deduce that MR3, like MR1, is satisfied.

As showcased in the examples, we assess the MRs' validity by comparing the expected and actual output traces of the follow-up test cases. The higher the similarity between the two traces, the higher the degree of satisfaction of the MR. In practice, we use a distance metric d to define an *MR-falsification degree* \mathcal{MF} :

$$\mathcal{MF} = d(G[r(t)](t), e(t)). \quad (1)$$

For example, in MR2, the follow-up input reference is $r(t) = \alpha \cdot r_x(t)$, and its expected output is $e(t) = \alpha \cdot G[r_x(t)](t)$. Then, to assess the validity of MR2, we compare $G[\alpha \cdot r_x(t)](t)$ with $\alpha \cdot G[r_x(t)](t)$. The lower the distance between the traces, the lower the degree of MR-falsification, the more the MR is satisfied. Ideally, when the MR is satisfied, we expect a zero distance, i.e., the actual and expected output traces are identical. In practice, however, small deviations are expected because of phenomena such as measurement noise or uncertainty in the system.

Finally, we note that MRs can be applied in sequence; i.e., MRs can be applied to input and expected output traces that were also obtained from MRs. This enables the generation of a wider variety of follow-up input traces with expected output traces. Furthermore, applying MRs in sequence does not require the actual output traces for the intermediate input traces to obtain the expected output. Indeed, the expected output can be derived by applying the MRs in the sequence to the initial output traces, thus avoiding the need to execute the CPS multiple times. For example, we can apply MR1 to two test cases where we previously apply MR2 and MR3, respectively. Such follow-up input trace $r_z(t)$ looks as follows:

$$r_z(t) = \alpha \cdot r_x(t) + r_y(t + \delta). \quad (2)$$

Then, we can compare the output to assess whether the MRs are satisfied or not:

$$\mathcal{MF} = d(G[r_z(t)](t), \alpha \cdot G[r_x(t)](t) + G[r_y(t)](t + \delta)).$$

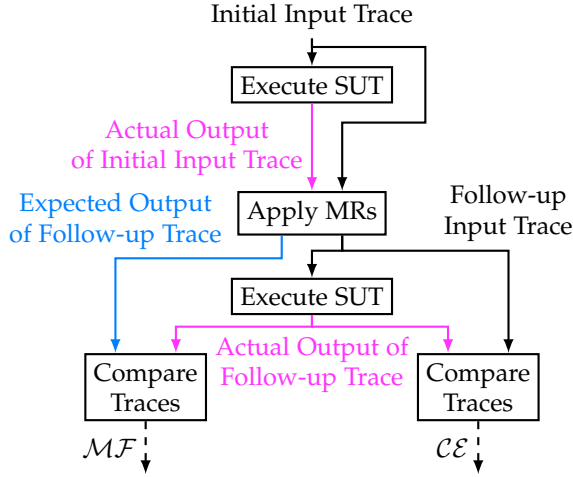


Fig. 4: Use of the metamorphic relations in the proposed approach. The boxes represent approach steps, solid arrows represent the tests’ input and output traces. Specifically, black arrows are the input traces, while the purple and azure arrows are the actual and expected output traces, respectively. The dashed arrows represent the distance metrics used to quantify the control error and the MR-falsification degree.

In this case, we can run only three tests, to obtain $G[r_x(t)](t)$, $G[r_y(t)](t)$ and $G[r_z(t)](t)$. We do not need to run tests to obtain the intermediate results for $G[\alpha \cdot r_x(t)](t)$ and $G[r_y(t + \delta)](t)$, to separately assess the validity of the application of MR2 and MR3, thus reducing the number of required CPS executions.

4 GENETIC PROGRAMMING BASED ON METAMORPHIC RELATIONS

We aim at generating input traces that falsify the MRs (i.e., test cases with high MR-falsification degrees), while avoiding trivial fails (i.e., test cases with large control error). Specifically, we use the MRs to modify and combine initial input traces and build follow-up input traces together with their associated expected output traces. Then, for the follow-up input traces, we can compute the control error (\mathcal{CE}) and MR-falsification degrees (\mathcal{MF}). Figure 4 shows how we use the MRs to both generate test cases and assess their control error and MR-falsification degrees. In this figure, the colours of solid arrows distinguish the input traces (black arrows), the actual output traces of the tests (purple arrows) and the expected output traces of the new tests (azure arrows). The blocks represent different steps: the incoming arrows are inputs to the blocks and the outgoing ones are their outputs. The “Execute SUT” blocks receive reference input traces and generate actual output traces. The “Apply MRs” block uses the MRs to manipulate pairs of input and output traces and generate follow-up input traces together with the associated expected output traces. In the right “Compare Traces” block, we compare the follow-up input and its actual output to compute the control error. In the left “Compare Traces” block, we compare the expected and actual outputs to assess whether the MRs hold or not for the given test cases (i.e., the

computation of Equation 1). The dashed arrows indicate the values obtained by the traces comparison.

To generate the input traces, we search the space of possible combinations of MRs applied to diverse initial input traces, i.e., the different ways to implement the “Apply MRs” block in Figure 4. To perform this search, we leverage Genetic Programming (GP). GP is an evolutionary approach that aims to search for the best program to perform a given task. GP evolves a population of individuals where each individual is a program and the ability of a program to perform the given task is called fitness. Like any evolutionary search algorithm, this population evolves over a number of generations through breeding (which entails crossover and mutation) and survival (selection of the fittest individuals).

Algorithm 1 outlines the main steps of the evolutionary search algorithm that we employ. The algorithm starts with the generation of the initial population (Line 1) composed of a user-defined number of individuals (`pop_size`). Then, the fitness of the initial population is assessed (Line 2) and the archive—which is the collection of the fittest individuals—is initialised with the fittest individuals of the initial population (Line 3). Afterwards, the main search loop (Line 5) starts, which is executed as many times as the allotted generations (`num_gens`). For each generation, a new set of individuals is created by breeding the current generation (Line 6). This includes mutation and crossover, which are usually applied based on user-defined probabilities. The offspring is then assessed (Line 7) and used to update the archive (Line 8). Finally, a subset of the offspring individuals is selected for survival and used to create the next generation (Line 9). After evolving the desired number of generations, the algorithm returns the archive with the fittest individuals to the user.

In our case, the objective is the maximisation of the MR-falsification degree while avoiding high control error. Thus, we define programs (i.e., individuals in search) that apply various combinations of MRs to different initial input traces and MRs parameters (i.e., the scaling value α when applying MR2 and the shift value δ when applying MR3). We now first delve into the details of our GP-based test case generation, and then discuss how we apply combinations of MRs to generate arbitrary input traces together with the associated expected output traces.

Algorithm 1 Evolutionary Search

Input: `pop_size`, `num_gens`

Output: archive

```

1: pop ← generateInitialPopulation(pop_size)
2: fitness ← assess(pop)
3: archive.update(pop, fitness)
4: i ← 0
5: while i < num_gens do
6:   offspring ← breeding(pop)
7:   fitness ← assess(offspring)
8:   archive.update(offspring, fitness)
9:   pop ← survival(offspring)
10:  i ← i + 1
11: end while
12: return archive

```

4.1 Genetic Program

4.1.1 Individual Representation and MR-Application Grammar

Our individuals are programs representing valid sequences of MRs applications. One of such programs starts from a number of initial input traces and returns a single input trace with an associated expected output trace. To apply MR2, it needs scaling values for the variable α —how much to scale the trace—and, to apply MR3, it needs shift values δ —how much to shift the trace in time. Accordingly, we identify three types of terminal symbols for the program grammar:

- r is an initial input trace,²
- α is a scaling value used to apply MR2, and
- δ is a shift value used to apply MR3.

Those terminal symbols are place-holders for actual input traces, scaling values, and shift values. Technically speaking, the input traces and values are the actual terminal symbols. For simplicity, we treat these place holders as the terminal symbols and implement them as *ephemeral constants*. Each instance of an ephemeral constant is assigned a random value upon the program creation and this value is kept for the rest of the search. In this way, different instances of the same terminal can have different values but from the point of view of the search they are still treated as constants.

Using these terminal symbols, we define the following syntax that represents the application of the MRs to arbitrary traces with arbitrary scaling or shifting values.

$$\begin{aligned} \langle P \rangle &::= \langle trace \rangle \\ \langle trace \rangle &::= r \\ &| \langle trace \rangle \oplus \langle trace \rangle \\ &| \alpha \bullet \langle trace \rangle \\ &| \delta \triangleright \langle trace \rangle \end{aligned}$$

This grammar states that any valid program $\langle P \rangle$ must return a trace. A trace $\langle trace \rangle$ can be a trace r in itself (potentially multi-dimensional), or it can be obtained from the application of one of the three MRs. The first MR, denoted by \oplus , generates a new trace from two traces $\langle trace \rangle$ and $\langle trace \rangle$. The second MR, denoted by \bullet , generates a new trace from a scaling value α and a trace $\langle trace \rangle$. The third MR, denoted by \triangleright , generates a new trace from a shift value δ and a trace $\langle trace \rangle$. The follow-up trace is then computed by applying the associated MR. As an example, the sequence of MR applications from Equation 2 can be written as the following program P :

$$P = (\alpha \bullet r_x) \oplus (\delta \triangleright r_y).$$

The output of this program is then the follow-up trace r_z of Equation 2.

4.1.2 Generation of Initial Population

We generate the initial population as a set of random programs with valid syntax. To prevent the generation of trivial programs (e.g., an individual that is just a terminal symbol, like $P = r$, thus not representing the application of any MRs) or unduly large programs, we respectively set a

2. For brevity, from now on we drop the time-dependency (t) of the traces.

minimum and maximum number of nested non-terminal symbols. This ensures that the number of applied MRs in an individual is bounded by minimum and maximum limits.

4.1.3 Fitness Assessment

The objective of the search is the maximisation of the MR-falsification degree while maintaining an acceptable control error. To capture this objective, we define a fitness function that grows linearly with the MR-falsification degree and is penalised exponentially by the control error when it exceeds a given threshold. For a given individual i , the fitness function is

$$\mathcal{F}(i) = \frac{\mathcal{MF}(i)}{b^{c(\mathcal{CE}(i) - \mathcal{CE}_{th})}}, \quad (3)$$

where $\mathcal{MF}(i)$ is the individual's MR-falsification degree, $\mathcal{CE}(i)$ is its control error, \mathcal{CE}_{th} is the threshold defining the maximum acceptable error, and b and c are user-defined constants. The MR-falsification degree is computed based on Equation 1, and the control error is the distance between the input reference and the actual output, thus

$$\mathcal{CE}(i) = d(r, G[r]). \quad (4)$$

When computing \mathcal{MF} and \mathcal{CE} , we want to assess how close the values of the expected and actual output traces are, at each point in time, and similarly the reference input and actual output traces, respectively. To quantify this distance, in our approach, we use the Euclidean distance (commonly used in previous CPS literature to compare traces [17]), which is the sum of the absolute values of the differences in trace values across time steps, and divide it by the length of the trace.³ Mathematically, for two traces a and b , with values a_k and b_k at a given time step k , we compute

$$d(a, b) = \sum_k |a_k - b_k| / k_{\max}, \quad (5)$$

where $|\cdot|$ represents the absolute value function, and k_{\max} is the number of samples of the traces. Using such metric, we can then use a threshold to assess whether two traces are similar or not. This distance can be interpreted as the average value difference between the two traces over time steps. For example, two traces with a distance of 5 means that, at each time step, they differ on average by 5 units.

4.1.4 Breeding: Mutation and Crossover

For the mutation and crossover operators, we employ standard solutions from the GP literature. When mutating an individual (program), we randomly select a terminal or non-terminal symbol. We then substitute it (and the symbols that it expands into) with a new randomly generated sub-program that returns a compatible symbol with the one removed. For example, in the program shown above, we could select \bullet and substitute it with the \oplus symbol and new randomly generated ephemeral constants. The program P is then mutated into P_{mut} , where the azure part is mutated into the purple one:

$$P = (\alpha \bullet r_x) \oplus (\delta \triangleright r_y)$$

3. Since all the traces are of the same length, the division by the length is not strictly necessary. However, it makes the metric equal to the average distance, thus enabling a more intuitive interpretation of the metric.

$$P_{mut} = (r_w \oplus r_j) \oplus (\delta \triangleright r_y).$$

Similarly, when performing a crossover, we randomly select a terminal or non-terminal symbol from one of the two individuals selected for reproduction. We then select (again randomly) a compatible symbol from the other individual, where compatible means that the two symbols can be swapped and we still obtain syntactically valid programs. The crossover is then performed by swapping the two symbols in the two individuals. An example of crossover is

$$P_1 = (\alpha_1 \bullet r_x) \oplus (\delta \triangleright r_y), P_2 = \alpha_2 \bullet (r_w \oplus r_j)$$

$$\rightarrow$$

$$P_3 = r_w \oplus (\delta \triangleright r_y), P_4 = \alpha_2 \bullet ((\alpha_1 \bullet r_x) \oplus r_j).$$

Here, the parents P_1 and P_2 generate the offspring P_3 and P_4 by swapping $(\alpha_1 \bullet r_x)$ with r_w : the symbols involved in the swap are highlighted in azure in the parents and in purple in the offspring.

When performing mutation and crossover, GP is often affected by bloating. Bloating is the uncontrolled increase of the size of individuals, which eventually cannot be managed by the executing platform. To prevent such occurrence, each time that mutation and crossover are performed, we assess the size of the new individuals. If their size (defined as number of symbols in the program) is beyond a set threshold, one of their parents is instead chosen to move to the new generation.

4.1.5 Selection Mechanism and Diversity

According to the GP algorithm, at each generation, we mutate and crossover the current population to create an offspring. Among the children in the offspring, we then select the fitter ones to be carried over to the next generation. For this selection, we use the standard selection tournament, where a given number of individuals (usually two or three) are randomly picked, and among those the one with the highest fitness is passed on to the next generation. This is repeated until enough individuals have been selected to form the new generation.

To avoid duplicates, before adding an individual to the new generation, we compare it with individuals that are already included in the next generation. We compare two individuals by measuring the Euclidean distance between the input traces that they generate, as for \mathcal{MF} and \mathcal{CE} in Equation 5. If the two programs generate input traces with a distance lower than a user-defined *similarity threshold*, we consider the two individuals to be similar, and we do not include the new one in the new generation. When an individual is considered a duplicate, we discard it and add instead a random individual from the archive. In this way, we avoid having similar individuals in each generation, thus maintaining population diversity.

4.1.6 Archive and Search Output

At the end of the search, we return to the user an *archive* containing the highest fitness individuals generated through the whole search. To avoid duplicates in the archive, we add a new individual to the archive only if it is sufficiently different from the ones it already contains. Like for the

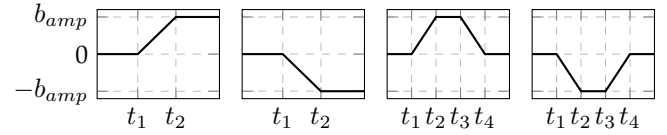


Fig. 5: The four different patterns used for the definition of the initial traces. Each pattern has a number of time parameters (the t_i indices) that are randomly selected when the ephemeral constant is created for a initial trace terminal symbol. In contrast, b_{amp} is fixed and set by the user to ensure that the initial trace belongs to the design scope.

diversity in the selection mechanism, we use the Euclidean distance to compare individuals, and the same user-defined threshold to assess if two individuals are too similar.

4.2 Generation of Valid Arbitrary Input Traces

We conclude the description of our approach by discussing how we generate values for the terminal symbols and apply combinations of MRs in practice. This is important as it affects both the effectiveness of the search as well as which traces can be generated with our approach. First, we want the initial input traces of a program to be within the design scope. In this way, the expected output trace of the program is representative of the CPS behaviour within the design scope, and the MR-falsification degree is then a measure of how far the follow-up input trace is from the design scope, thus effectively guiding the search.⁴ Second, we want our approach to be able to generate varied and arbitrary input traces within a user-defined valid input range. The use of this valid input range allows users to avoid large input values that are not relevant to the CPS under test. This also ensures that the application of the MRs generates input traces with values within the valid input range.

4.2.1 Generation of Initial Input Traces

We ensure that the initial input traces (i.e., the ephemeral constants of the terminal symbol r) are within the design scope by using simple input patterns and small amplitude values. As discussed in our previous work [2], simple patterns and especially small amplitudes are not expected to falsify the linearity assumptions. Intuitively, in a CPS, a short and slow movement is simpler to handle than a long and fast one. We use the patterns shown in Figure 5 with a fixed user-defined amplitude b_{amp} . To guarantee that the initial inputs are within the design scope, b_{amp} can be appropriately chosen. The patterns include linear increments and decrements of the values. The idea is that by applying a combination of the MRs to an adequate number of such

4. Technically speaking, even if we consider initial input traces that are out of the design scope, the MR-falsification is still a valid metric of how much a combination of MRs is falsified. However, the \mathcal{MF} metric would no longer be a “distance from the design scope”, since the expected output is already outside of the design scope. This would limit the search ability to avoid tests that are trivial fails (i.e., with large control error). In fact, tests further out of the design scope are likely to be trivial fails. Hence, only when initial input traces are within the design scope, the MR-falsification degree helps the search target the right compromise between avoiding trivial failures and effectively falsifying the MRs.

initial traces, we can, in theory, approximate any arbitrary trace. If the CPS does not perform well with these proposed patterns, it indicates that there are some fundamental issues with the CPS design. This further suggests that it is too early in the development to start testing with more complex traces. For example, if a drone is not able to move for one meter in a straight line, it is too early to test it with more complex or longer sequences. The parameters t_1 , t_2 , t_3 and t_4 are randomly selected each time an ephemeral constant is generated for the initial input trace symbol r . By allowing different values for such parameters, we enable the generation of diverse initial input traces that can then be combined with the MRs and generate more complex follow-up traces. As visible from Figure 5, the initial input traces are centred around zero. In practice, before feeding the input traces to the SUT, we apply an *input bias* that shifts them in the middle of the user-defined valid input range. In this way, the patterns can be seen as deviations from the input bias rather than absolute values. This allows us to guarantee that all initial input traces are valid (as long as b_{amp} is within the valid range) and to treat cases where the valid input range is not centred around zero in the same way as cases where it is.

4.2.2 Implementation of MR2 to Cover the Valid Input Range

To generate input traces within the valid input range, we use the amplitude scaling of MR2, since the initial input traces have a fixed amplitude. However, at the same time, we need to ensure that we do not exceed the valid input range. This implies that the maximum allowed value for the scaling depends on the amplitude of the trace that it is applied to. For example, if the user-defined valid range is between 2 and -2, and the maximum and minimum values of the trace that we are applying the MR to are 1 and -0.5, then the set of allowed scaling values that will not generate an invalid trace is between 0 and 2. However, if the maximum value of the trace was 2, then the maximum scaling value would be 1. To make sure that we can both cover the valid input range but also that we do not exceed it, we use for the symbol α a value scaled between 0 and 1. Then, when we apply MR2, we first compute the set of valid scaling values for the given trace and then use the α value to select the actual scaling value from this set. In the example above, with valid scaling values between 0 and 2, an α value of 0.5 would lead to the selection of the actual scaling value of 1, and 0.33 would lead to the selection of 0.66.

For some corner cases, when the trace to which the MR is applied has only small values, the set of valid amplitude scaling values can include some very large ones. For example, in a drone, if the maximum value of the trace is 0.001 m and the maximum valid amplitude value is 2, the maximum allowed scaling value is 2000. While this is correct and will generate valid inputs, it can cause problems when computing the expected output. In fact, if the output of the initial trace has even a small deviation (e.g., because of some noise in the sensors), when scaled by a large value, this deviation will be amplified. For example, a deviation by 0.01 m, that can be expected because of noise, might be scaled by 2000, and generate an expected output that is in the range of 20 m, while the reference is still within

2 m and -2 m. This is technically correct and can help detecting unexpected CPS behaviours—in the example, it would highlight that the 0.01 m initial deviation was not expected—but, due to the large deviation of the expected output, it can generate individuals with such a high fitness that the search will focus solely on them. Indeed, given the large deviation of the expected output from the reference, the fitness of these individuals can be orders of magnitude larger than the other individuals. To avoid such extreme cases, we limit the actual scaling values to the ratio between the maximum allowed amplitude and the amplitude of initial traces. In the drone example with maximum amplitude of 2 m, if b_{amp} was 0.02 m, then we would limit every scaling value to 100. With this rule of thumb, we can thus generate all the inputs within the allowed range but avoid extreme amplitude scaling values.

4.2.3 Implementation of MR1 and MR3 to Generate Diverse Patterns

To obtain input traces with more varied and arbitrary patterns, we leverage MR1 and MR3 to combine the initial input traces. MR1 combines different traces by summing them, and thus can effectively create new arbitrary patterns. However, when applying MR1 to two traces, the amplitude values of the new trace will likely increase and might exceed the valid range. To make sure that MR1 does not generate inputs that are out of the valid range, we always apply it in combination with MR2 and divide by 2 the new trace. In this way the new trace is always within the same range of values as the original traces and cannot violate the user-defined range. Finally, while MR3 in itself does not alter the pattern of a given input to which it is applied (the trace is only shifted in time, and the values do not change), it enables the combination, through MR1, of two traces in different ways by using different shift values. This synergy between MR3 and MR1 provides an extra degree of freedom to the search algorithm when combining two traces. As a result, we can rely less on the variety of initial input traces and leverage more the search algorithm for exploring the space of possible input traces.

5 EMPIRICAL EVALUATION

Our approach aims at generating input traces, together with the associated oracles, and the objective of falsifying the MRs. Accordingly, in our empirical evaluation, we assess our contribution both to the oracle problem and to the generation of such input traces. First, we assess whether the GP search is actually needed as well as its effectiveness at generating non-trivial traces that falsify the MRs. Second, we assess the ability of the MRs to extend the state of the art (i.e., methods based on the control error) as oracle for CPSs. We formulate the objectives of our experiments with the following Research Questions (RQs):

RQ1: How does the GP search compare to a baseline based on random generation of programs?

With this RQ, we assess the GP search part of the proposed test case generation approach, i.e., its ability to generate input traces that falsify the MRs but are not trivial fails. We compare the achieved fitness against the random generation of programs in order to assess the need for an evolutionary

TABLE 1: Parameters required for the implementation of the MRs for each test subject based on our engineering guidelines.

Parameter	Values CF	Values ET
Tests duration	10	50
Minimum start time	3	1.5
Initial amplitude	(0.2,0.2,0.2)	500
Amplitude range	$x, y: (2,-2)$ $z: (0.5, 1.2)$	(6000,1200)

algorithm. In this way, we can assess how difficult it is to falsify the MRs while avoiding very large control error values (i.e., trivial fails).

RQ2: Is the MR-falsification metric improving the oracles in comparison to the use of control error?

With this RQ, we evaluate whether the MR-falsification metric provides engineers with new information when compared to the sole use of the control error. Specifically, we are interested in assessing whether, for similar control error values, we obtain different MR-falsification values. If so, the MR-falsification metric offers engineers a new mechanism to distinguish between passed and failed test cases.

Before addressing our RQs, we present the test subjects and the settings chosen for the GP.

5.1 Test Subjects

We chose them as they are CPS developed with the use of linear systems theory and commonly found in daily life. CF is a drone used both in robotics [18] as well as in software testing research [19, 2]. We rely on a CF simulation model from previous research, which consists of a simulator of the physical drone flying in space, connected in closed-loop with a python implementation of the control software. It receives as input the desired position expressed as the three coordinates x , y , z , and it simulates how the control layer interacts with the physics to bring the drone to the desired position.

Our second test subject (ET) controls the revolutions per minute (rpm) of an engine.⁵ Here, the software controls the fuel injection to bring the engine speed to the desired one. The simulation model used for the testing is developed by Mathworks and is implemented in Simulink, a wide-spread tool for the development of CPS.

5.2 Parameter Settings

The application of our testing approach requires setting parameters for (i) the implementation of the MRs, and (ii) the GP algorithm.

5.2.1 Setting MR Implementation Parameters with Guidelines

Table 1 lists the parameters that need to be set for the MRs implementation together with the values chosen for our test subjects. These parameters have a quantifiable impact on the approach implementation for a given test subject; thus we can provide and use a rationale for their setting. We provide the following guidelines to set them:

⁵ mathworks.com/help/simulink/slref/engine-timing-model-wit-h-closed-loop-control.html

TABLE 2: Parameters of the GP set with guidelines and manual tuning. We use the same values for both test subjects.

Parameter	Value
Algorithm	(μ, λ)
μ	50
λ	80
initial population size	μ
crossover rate	0.35
mutation rate	0.35
tournament size	2
number of generations	40
max nodes	300
max individual depth	8
min individual depth	4
min and max depth of mutated subtrees	(2,4)

TABLE 3: Control error and similarity thresholds used for both test subjects.

Parameter	CF	ET
Control error threshold	0.15	75
Similarity threshold	0.2	300

- **Test duration:** Selecting the test duration involves a trade-off between testing effectiveness and cost. The tests should be as short as possible to reduce testing cost, but long enough to allow the CPS to perform manoeuvres of interest. For example, for the delivery drone, the duration should be comparable to the time required to fly between a couple of way-points of the planned path.
- **Warm-up time:** This parameter sets a warm-up time for the CPS to reach a state where the actual test can start (e.g., a drone has to take off). In practice, it sets an initial time in which the input is fixed to the input bias (defined in Section 4.2) so that the CPS can reach that state. It can be set by analysing a test that inputs only the bias, observing how long it takes for the CPS to get ready for testing, and at the same time be kept as small as possible to minimise testing time. For the drone, this would be the time that it takes the drone to take off at the beginning of each test.
- **Initial amplitude:** This parameter sets the amplitude values for the base test cases. It should be small enough such that the CPS is expected to process it with the expected performance (e.g., speed), that is be within the design scope.⁶ At the same time, it should be large enough to actually perform a manoeuvre. In our delivery drone example, it should be large enough for the drone to actually move but small enough such that the initial test is within the design scope.
- **Amplitude range:** This parameter sets the valid value range for each input trace. It can be set according to the maximum values that the CPS is required to handle. In the drone, this could be the size of the space that the drone is supposed to fly in.

⁶ The details of the relation between input amplitude and design scope is discussed in previous work introducing the design scope [2].

TABLE 4: Results of the empirical investigation of the fitness function coefficients. The results include the average MR-falsification and control error.

CF	b					
	1.5		e		10	
	\mathcal{CE}	\mathcal{MF}	\mathcal{CE}	\mathcal{MF}	\mathcal{CE}	\mathcal{MF}
c 3.33	0.681	0.677	0.283	0.311	0.136	0.131
6.66	0.324	0.335	0.146	0.160	0.084	0.073
33.33	0.112	0.124	0.053	0.033	0.049	0.023

ET	b					
	1.5		e		10	
	\mathcal{CE}	\mathcal{MF}	\mathcal{CE}	\mathcal{MF}	\mathcal{CE}	\mathcal{MF}
0.007	77.28	22.36	166.01	111.62	85.50	43.75
c 0.013	126.41	65.52	94.46	48.56	48.73	23.13
0.066	56.03	24.73	31.76	8.86	21.91	3.63

5.2.2 Setting of Search Parameters

Setting the parameters for a search algorithm is a problem extensively studied in the literature. It has been observed that there is no unique answer to such problem, which largely depends on the specific application [20]. For this reason, based on existing guidelines [20], we use manual tuning to find a working set of values for the GP search. Table 2 reports the parameters that we set in this way together with the corresponding values. For these parameters, we used the same values across both test subjects.

The remaining parameters are specific to our search problem and need to be set for each application. Those parameters include the coefficients of the fitness function (the exponential base b , the exponent scaling coefficient c , and the control error threshold \mathcal{CE}_{th}), and the similarity threshold (Section 4.1.5) used to compare individuals. The control error threshold defines the control error value above which we consider a test to be a trivial fail (and fitness is exponentially penalised above this value). It represents the maximum accepted average distance between the actual output and the reference input. Since we expect CF to reach a position with an accuracy in the order of centimetres, we consider more than 0.15 m in average distance from the reference position to be a trivial failure. Since we expect ET to track the reference speed with an accuracy higher than hundreds of rpm, we consider more than 75 rpm in average distance from the reference rpm to be a trivial failure. The similarity threshold defines instead the minimum Euclidean distance below which two input traces are considered too similar and thus redundant. Similarly to the control error threshold, this parameter is also connected the expected accuracy of the CPS in tracking an input. Intuitively, the more accurate the CPS is expected to be, the more small input differences affect it. Thus, for the similarity threshold, we use larger values than the control error threshold to make sure that the difference between two traces is relevant when compared to the expected precision. Specifically, we use 0.2 m for CF and 300 rpm for ET. Table 3 summarises the threshold values chosen for our test subjects.

The remaining coefficients to be tuned are the two coef-

ficients of the fitness function: the base b of the exponential and the scaling factor c in the exponent of Equation 3. These parameters implement the trade-off between the control error and MR-falsification. However, it is difficult to quantify a priori their impact on the search. For this reason, we perform an empirical evaluation to set them. We perform such evaluation in three steps: (i) we define different sets of candidate values, (ii) we run experiments with the chosen sets of values, and (iii) we compare the individuals in the archive in terms of average control error and MR-falsification and select the set of parameters that achieve the best MR-falsification while maintaining the control error below a specified threshold. \mathcal{CE}_{th} .

For the base b , we include two alternatives frequently used in the literature, e and 10, together with a smaller value of 1.5. The coefficient c is a scaling factor for the control error contribution. Since the control error contribution depends on the unit of measure, it can have very different values in different applications (e.g., 0.15 m in CF and 75 rpm in ET). Thus, we adjust it to the control error range and avoid making the exponential function always very large or very small. Specifically, we use three values of c so that $c \cdot \mathcal{CE}_{th}$ equals 0.5, 1, and 5. Table 4 shows the results of the tests runs for each test subject: each row corresponds to a value of c and each column to a value of b . In the table, we highlight in purple the results that achieve the best \mathcal{MF} while maintaining the \mathcal{CE} below the threshold. For the evaluation, we use the parameters used to obtain those results.

5.2.3 Assessment of Search Random Variability

Since the results can be affected by the random nature of meta-heuristic search, we repeat the experiments with the chosen parameters to assess the impact of randomisation on the algorithm. We repeated the execution of our approach ten times (on top of the one execution used for the parameters assessment) with different seeds for the random number generator and compare the control error and MR-falsification values with the purple ones from Table 4. We then assess if the results present significant variance. For CF, in the 10 runs, we observe $\mathcal{CE} = 0.156 \pm 0.05$ and $\mathcal{MF} = 0.169 \pm 0.08$. For ET, instead, we observe $\mathcal{CE} = 54.36 \pm 17.6$ and $\mathcal{MF} = 24.9 \pm 12.3$. We desirably observe a small variation in the metrics' values, thus desirably showing a limited impact of randomness on our approach execution. For answering our research questions, we use the experiments selected from the results of Table 4.

To conclude, we note that further tuning of the aforementioned parameters might improve the performance of our approach. However, our current settings have already enabled us to convincingly and clearly support our conclusions. Therefore, we do not report additional experiments to optimise these values.

5.3 RQ1: Search Effectiveness

5.3.1 Methodology

To assess the effectiveness of our search algorithm, we compare it to a baseline that relies on random generation. More precisely, this baseline consists of the random generation of programs using our proposed grammar. To make the

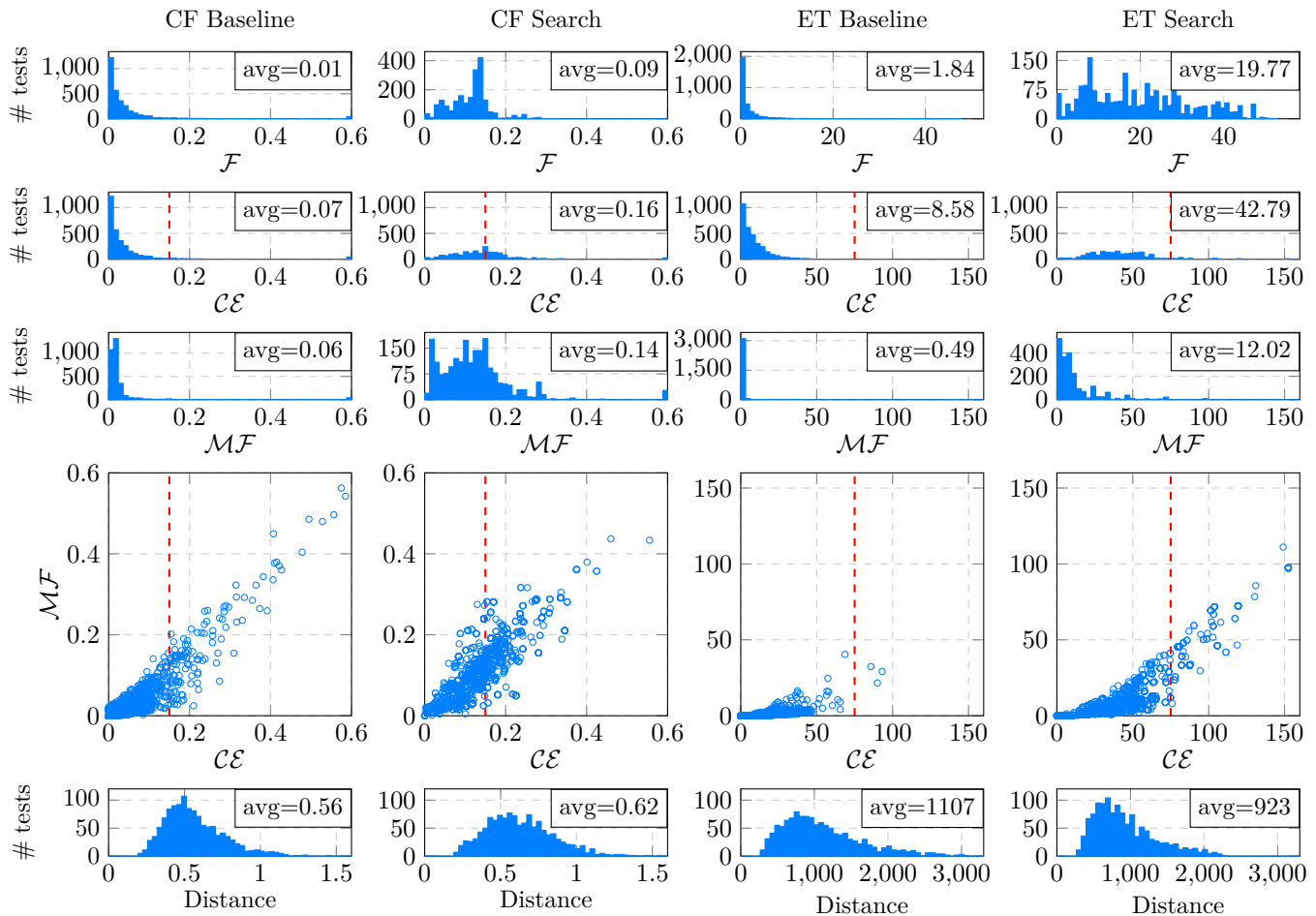


Fig. 6: Results of the experimental campaign. Each column of plots refers to a test subject (CF and ET) and test generation approach (baseline and search). Each row of histograms respectively reports the fitness \mathcal{F} , control error \mathcal{CE} , MR-falsification \mathcal{MF} , and distance. The scatter plots show the control error and fitness for each test. The red dashed lines indicate the control error threshold \mathcal{CE}_{th} .

results comparable and fair, we generate as many programs as the search generates across all generations, which is the number of generations multiplied with λ . This corresponds to generating $40 \cdot 80 = 3200$ random programs. We then compare the tests generated by the search and the baseline in terms of fitness \mathcal{F} , control error \mathcal{CE} , and MR falsification \mathcal{MF} . Fitness values show the effectiveness of the search and the baseline, while MR falsification and control errors capture the effectiveness of the test inputs generated by the search and the baseline. To visualise the comparisons across generated programs, we use histograms of the three metrics, reported in the first three rows of Figure 6 for each test subject and search configuration. The plots in the two left-hand columns of Figure 6 report the results for CF, respectively for the baseline and the search. In the same way, the plots in the right-hand columns report the results for ET. For CF, MR-falsification and control error can reach very high values, in some of the trivial failures as the drone flies very far from both reference and expected output. Specifically, the drone flies up to tens of meters away from the reference and expected output, which is very large compared to the expected precision in the order of centimetres. Such tests are not relevant for our analysis thus we limit the plots to

lower values.⁷ We also provide histograms of the Euclidean distances among the tests from the archive to assess whether the search is managing to generate diverse tests, and thus diverse ways to falsify the MRs.

In addition to the histograms, to assess the search performance, we study the relation between control error and MR-falsification for individual tests. To compare the two metrics, in the bottom row of Figure 6, we provide scatter plots of the control error and the MR-falsification where each observation is a test. We include all the tests across generations for the search algorithm and all of the random tests generated for the baseline. We also display a dashed red line indicating the control error threshold \mathcal{CE}_{th} . Since the objective of the search is to maximise MR-falsification while keeping the control error below this threshold, relevant high fitness individuals are the ones to the left of the dashed line and further up in the scatter plots.

⁷ The tests with large \mathcal{CE} and \mathcal{MF} are counted on the right-most part of the histograms. As it can be seen in the plots, they constitute a small minority of the overall number of tests.

5.3.2 Analysis

The fitness histograms in Figure 6 clearly show that the search generates tests with much higher fitness than the baseline—for CF the average fitness increases from 0.01 to 0.09, and for ET it increases from 1.84 to 19.77. By comparing the control error and MR-falsification histograms, we observe that, when using the search, they also increase in value, indicating that our approach outperforms the baseline by achieving higher MR-falsification values at the cost of an acceptable control error increase. Furthermore, it also confirms that maximising MR-falsification while constraining the control error is not a simple problem that can be addressed by random generation. From a diversity point of view, we observe in the distance histograms (the fourth row) small differences between the baseline and the search. Since the baseline is purely exploratory, this confirms the effectiveness of the proposed mechanism for fostering diversity during the search (Section 4.1.5).

By comparing our two test subjects, we observe that they exhibit different testing challenges. Looking at the scatter plots of CF, we observe that the baseline is already able to generate a number of tests with both high control error (above the threshold) and MR-falsification: such tests are the ones further up and right in the plot. In contrast, for ET, the baseline generates mostly tests with low control error (below the threshold) and MR-falsification. This happens because it is easier to cause a failure in CF, whereas ET is a more robust system. Intuitively, when a drone starts to misbehave, it may crash and irreparably fail, thus showing high control error and MR-falsification values. An engine, instead, even after showing a deviation from the expected behaviour, is much more likely to recover and return to its nominal behaviour. When it is easier to lead a system out of its design scope, like CF, the challenge is to cause nontrivial failures that cannot be detected by solely relying on control error. For such CPSs, our testing approach, using MR-falsification, enables the generation of more subtle failures, with low control error (below \mathcal{CE}_{th}) but out of the design scope (i.e., unexpected behaviour). With a more robust system, like ET, simply causing failures is a challenge. In this case, the search finds scenarios with higher MR-falsification than random generation, which necessarily also increases the control error—the tests are further up—but also further right in the scatter plot. Our tests thus show that MR-falsification is also a valid fitness metric to guide test generation for ET, as it can find tests with higher control error but still avoids trivial fails.

Summary: Our experiment results indicate that our approach significantly outperforms the baseline, achieving higher MR-falsification and acceptable control error. Specifically, we observe that satisfying the conflicting requirement of maximising the MR falsification while constraining the control error is a challenging problem. For CF, even though the baseline was also able to generate some failures, our approach increased the average MR-falsification values by more than two-fold (from 0.06 to 0.14), while keeping the average control error at 0.16, thus very close to the threshold $\mathcal{CE}_{th} = 0.15$ m. For ET, even though the system is robust and failing test cases are difficult to generate, the MR falsification was effective in guiding the search of test cases, not only

with higher MR-falsification degree but also higher control error. Notably, when compared to the baseline, the average control error increased from 0.49 to 42.79, thus still well below the threshold $\mathcal{CE}_{th} = 75$ rpm.

5.4 RQ2: Effectiveness of MRs as Oracle

5.4.1 Methodology

To assess the ability of MR-falsification to improve oracles based on the control error, we analyse whether, among those that show control error values below the threshold \mathcal{CE}_{th} (thus excluding trivial fails), the metric helps distinguish passed and failed tests. Specifically, we want to show that MR-falsification provides new information with respect to the control error. We study the two metrics in relation to one another in two ways: one quantitative and one qualitative. From the quantitative side, we use the coefficient of determination (also known as R-squared). This metric measures how much variance in one variable can be explained by another variable. R-squared is computed based on the residuals (i.e., the differences) that remain after performing a linear regression between \mathcal{MF} and \mathcal{CE} . It is normalised so that a value close to 1 indicates a strong relation between the two variables and 0 indicates no relation. To give a graphical interpretation, we are assessing how much a linear regression can explain the datapoints in the bottom plots of Figure 6 on the left-hand side of the red dashed line (the control error threshold). This allows us to quantify how strong the relation is between the two variables for tests with control error below the threshold. From the qualitative side, we analyse the MR-falsification and control error scatter plots in Figure 6. We use this to observe trends in the relation between the two metrics.

5.4.2 Analysis

On the quantitative side, we measure a R-squared value for CF and ET of 0.48 and 0.5, respectively. This means that the control error can explain approximately half of the variance that we observe in the MR-falsification. The other half is then new information available to the engineers to distinguish the passed and failed test cases. This shows that the MR-falsification metric improves oracles based on the control error, by allowing engineers to distinguish test cases within and outside of the design scope.

On the qualitative side, the bottom plots of Figure 6 confirm that MR-falsification has higher variance for tests below the control error threshold (highlighted by the red dashed line). The variation in MR-falsification values is clearly wider for the tests obtained using the search when compared to those of the random baseline. This is consistent with the answer to RQ1 that showed how the generation of non-trivial tests, which also falsify the MRs, requires a targeted search. Thus, when the test generation does not explicitly target the MR-falsification, as in the baseline, fewer tests with different MR-falsification values are observed.

When looking at the complete scatter plots, i.e., including the tests above the control error threshold, they seem to show that the MR-falsification is linearly correlated to the control error and thus does not provide new information. This is expected for tests with larger control error, since the MR-falsification and control error measure the deviation

of the actual output from the expected output and the reference, respectively. Since the expected output effectively tracks the reference (recall that the base test cases are designed to be well within the design scope), when the actual output largely deviates from one of them, it will also deviate to a similar extent from the other. However, when focusing on tests with control error below the threshold, we observe more spread in MR-falsification values for the same control error value. This confirms the weaker relation between the two variables, as we observed also with R-squared analysis. Furthermore, we qualitatively observe that, below the threshold, the spread of MR-falsification values increases as the control error increases. In other words, tests with lower control error tend to have similar MR-values. This is also expected as such tests are most likely well within the design scope, as the CPS effectively tracks the reference, thus leading to low MR-falsification values.

Summary: Our tests show that MR-falsification effectively supports engineers in distinguishing test cases that show unpredictable behaviour of the CPS, though they are not trivially failing (acceptable control error). Engineers have thus one more mechanism to their disposal, in addition to the control error, to identify tests that show unpredictable behaviour. Furthermore, our tests show that this information is available in the range of control error values where it is most needed: when they are neither very low (i.e., tests that clearly show desirable behaviour of the CPS) nor too high (i.e., tests that clearly show failures of the CPS).

5.5 Limitations and Threats to Validity

In terms of internal validity, we identify a threat concerning the statistical analysis of the relation between MR-falsification and control error. The relation analysis between MR-falsification and control error is limited by the impossibility of obtaining unbiased, sufficiently large samples of either of the quantities. Specifically, we cannot generate input traces where we know a priori the control error (or the MR-falsification). Thus, the analysis is limited by the fact that it is difficult to generate test cases with diverse MR-falsification values (as observed in RQ1). Despite this, our statistical comparison results align with our visual inspection findings. Our analysis shows that there is not a strong relation between the two quantities when considering the tests with control error below the threshold, which is where we are interested in providing a new metric to distinguish passed and failed test cases.

External validity concerns the generalisability of our results to other CPSs. We successfully applied our approach to two CPSs from the automotive and drone domains, thus there might be threats to the approach's applicability to CPSs from other domains. However, the fundamental component of our approach, the MRs, are based on the definition of a linear system, which is common to any CPS that is developed with the use of control theory and is independent of the specific application domain. Thus, our approach is, in principle, applicable to any CPS that is developed leveraging control theory.

The practical applicability of our approach might be limited by two main factors. First, the need to tune the parameters of the fitness function: in our two test subjects,

we needed to use different values for these parameters (Table 4). When applying our approach to other CPSs, some iterations for choosing these values might be needed, thus increasing the number of tests to be performed and thus the testing cost. On the other side, even a small campaign like the one we performed, based on standard values, was able to provide effective parameters. This suggests that the tuning of the fitness function parameters should not be a major limitation. Second, the proposed setup for the search requires a significant number of tests for the approach application (namely, $40 \cdot 80 = 3200$ tests). This can be limiting for CPSs that require long execution time to test. Reducing the execution time is outside the scope of our study. However, for our experimental campaign, we did not perform any further optimisation of the search parameters after determining the values listed in Table 2. Therefore, it is likely possible to reduce the number of individuals or generations, thus reducing the number of required CPS executions (tests) required by our approach.

5.6 Availability of Results

The code implementing our approach and the test subjects is available through the following private link:⁸

- <https://figshare.com/s/37ea7c7f8a3ce1eee6c2>.

The data of the tests for the drone and engine are available here:

- CF: <https://figshare.com/s/bf8da4d28ea594e90ee2>,
- ET: <https://figshare.com/s/d77ed6916dd0273b4091>.

6 RELATED WORK

The oracle problem for CPSs is not new in the software engineering literature. Several specification languages and associated runtime verification tools have been proposed to specify CPS requirements as oracles [21]. Kapinski et al. [22] provide a library of common CPS behaviours, including steady-state error and overshoot (mentioned in Section 1); notably, the authors also provide templates for expressing such properties in STL [23]. Boufaied et al. [21] proposed a taxonomy of CPS properties (like the overshoot mentioned in Section 1) and reviewed the expressiveness of various signal-based temporal logics in terms of the property types identified in the taxonomy. Menghi et al. [24] as well as Dawes and Bianculli [25] proposed specification languages for expressing hybrid properties of CPSs, capturing both the software and the physical behaviour. Several approaches have proven the practical applicability of specification-driven runtime verification tools to the oracle problem in the CPS domain, both in offline [24, 26, 27] (in the aerospace domain) and online settings [28] (in the automotive domain). Our approach, differently from these works, does not discuss the satisfaction of the requirements, but rather the satisfaction of the design assumptions expressed as MRs.

Few works on CPS testing use concepts from control engineering. The most closely related work is from Hildebrandt et al. [8], as the authors seek to generate subtle (i.e., non-trivial) failures in trajectories of mobile robots (i.e.,

8. Should the article be accepted, we will publish the code in a long-term, archival repository.

in the jargon of this article, sequences of input position references). The authors use models of the physics (the same ones used during the development of control algorithms) to compute the set of feasible input traces and then use user-defined stress metrics to guide the test-generation process. In this work, we instead use the MR-falsification degree as a new (stress) metric and the control error threshold to target non-trivial failures. This makes our approach more general and application independent. He et al. [29] used system identification [30] (a sub-field of control engineering) to implement oracles for CPS output traces. Other works connect to control engineering aspects of CPSs by expanding temporal logics with frequency-domain operators [31, 32]. The frequency domain is widely used in traditional control engineering as alternative to the time domain to represent systems and signals, as it is well-suited to analyse equation-based models of the physical world. While such works move toward bridging the gap between software and control engineering in CPSs, none of them integrates the guarantees that can be obtained from the two disciplines. One of the main strengths of our approach is the use of the design assumptions to achieve such synergy.

CPS requirements expressed in signal-temporal logic have been also used to guide the generation of CPS test cases [7]. Such works fall under the class of CPS-falsification techniques. Notably, Zhang et al. [7] discuss the relevance of finding subtle requirements violations. Among falsification approaches, we highlight two prior works that leverage control engineering tools, and more specifically system identification [30]. In such works, system identification techniques are used to reduce the number of tests that have to be executed in order to find faults [33] or to reduce the parameter definition effort required by genetic algorithms [34]. However, these approaches, while they do leverage control theoretical tools, they still target the falsification of the requirements. Differently, we use the control theoretical models to define a metric (the MR-falsification) to guide the test case generation, thus as part of the testing objective itself.

Very early work in the MT literature investigated its applicability to CPSs, specifically control systems [35]. More recent work applied MT to an elevator system, using MRs concerning the system performance and quality of service [36, 12, 37]. Li et al. [15] performed a preliminary exploration of MT applicability to multi-module UAVs, using hand-written MRs. Deng et al. [13] applied MT to autonomous driving using MRs derived from traffic rules and domain knowledge. Finally, Ayerdi et al. [14] used MRs to perform runtime verification of autonomous driving systems. In contrast, our work clearly departs from the above works by defining the MR using the design assumptions, instead of requirements satisfaction. Notably, by using assumptions that underlie any control-theoretical model, we define MRs that are applicable to any CPS from any domain, as long as it is developed based on control theory.

7 CONCLUSIONS

We addressed the problem of generating CPS input traces with potentially arbitrary shapes together with associated

oracles. Since CPS requirements are defined only for simple input traces, we instead used the concept of design assumptions – in fact, when the design assumptions hold, engineers can rely on the control theoretical guarantees on the CPS performance. Specifically, we used the linear behaviour design assumption to define MRs that can be used for the generation of new input traces with associated expected output traces. We then set out to search for input traces that falsify the MRs while avoiding trivial failures. To perform this search, we defined a grammar for programs representing the possible combinations of MR applications. Using this grammar, our GP-based approach searches for input traces that falsify the MRs while avoiding large control error (associated to trivial failures).

We evaluated our testing approach on two test subjects: a drone and an engine. Our results show, first, that falsifying the MRs while avoiding trivial failures is a complex problem. Second, they show that the MRs falsification complements the use of the sole control error for identifying passed and failed test cases. Specifically, in test cases where the control error is not decisive (i.e., test cases where the control error value is not large enough to clearly identify a failure), MR falsification shows different values. Such difference allows engineers to distinguish test cases that do or do not satisfy the design assumptions.

In future work, we will use the MRs to address the test case generation in combination with other testing objectives. For example, if coverage criteria are available, then the MRs can be used to generate test cases that optimise the given criterion. Thanks to the MRs, we can then associate oracles in the form of expected outputs to the generated test inputs. Furthermore, we will address the testing of other design assumptions among the ones listed in our previous work [2]. The remaining assumptions concern the interaction with discrete inputs, the validity of the physics models, and implementation aspects such as real-time execution and numerical precision.

ACKNOWLEDGMENTS

This project has received funding from SES and the Luxembourg National Research Fund under the Industrial Partnership Block Grant (IPBG), ref. IPBG19/14016225/INSTRUCT. Lionel Briand was partly funded by the Science Foundation Ireland grant 13/RC/2094-2 and NSERC of Canada under the Discovery and CRC programs.

REFERENCES

- [1] E. A. Lee, "The past, present and future of cyber-physical systems: A focus on models," *Sensors*, vol. 15, no. 3, pp. 4837–4869, 2015.
- [2] C. Mandrioli, S. Y. Shin, M. Maggio, D. Bianculli, and L. Briand, "Stress testing control loops in cyber-physical systems," *ACM Trans. Softw. Eng. Methodol.*, vol. 33, no. 2, dec 2023. [Online]. Available: <https://doi.org/10.1145/3624742>
- [3] K. J. Astrom and R. M. Murray, *Feedback Systems: An Introduction for Scientists and Engineers*. USA: Princeton University Press, 2008.

- [4] J. P. Hespanha, *Linear Systems Theory*. Princeton, New Jersey: Princeton Press, Feb. 2018, ISBN13: 9780691179575.
- [5] A. Calanca, R. Muradore, and P. Fiorini, "A review of algorithms for compliant control of stiff and fixed-compliance robots," *IEEE/ASME Transactions on Mechatronics*, vol. 21, no. 2, pp. 613–624, 2016.
- [6] I. Lopez-Sanchez and J. Moreno-Valenzuela, "Pid control of quadrotor uavs: A survey," *Annual Reviews in Control*, vol. 56, p. 100900, 2023. [Online]. Available: <https://www.sciencedirect.com/science/article/pii/S1367578823000640>
- [7] C. Zhang, P. Kapoor, R. Meira-Goes, D. Garlan, E. Kang, A. Ganlath, S. Mishra, and N. Ammar, "Investigating robustness in cyber-physical systems: Specification-centric analysis in the face of system deviations," 2024. [Online]. Available: <https://arxiv.org/abs/2311.07462>
- [8] C. Hildebrandt, S. Elbaum, N. Bezzo, and M. B. Dwyer, "Feasible and stressful trajectory generation for mobile robots," in *Proceedings of the 29th ACM SIGSOFT International Symposium on Software Testing and Analysis*, ser. ISSTA 2020. New York, NY, USA: Association for Computing Machinery, 2020, p. 349–362. [Online]. Available: <https://doi.org/10.1145/3395363.3397387>
- [9] T. Y. Chen, S. C. Cheung, and S. M. Yiu, "Metamorphic testing: A new approach for generating next test cases," 2020.
- [10] T. Y. Chen, F.-C. Kuo, H. Liu, P.-L. Poon, D. Towey, T. H. Tse, and Z. Q. Zhou, "Metamorphic testing: A review of challenges and opportunities," *ACM Comput. Surv.*, vol. 51, no. 1, jan 2018. [Online]. Available: <https://doi.org/10.1145/3143561>
- [11] J. Ayerdi, V. Terragni, G. Jahangirova, A. Arrieta, and P. Tonella, "Genmorph: Automatically generating metamorphic relations via genetic programming," *IEEE Transactions on Software Engineering*, p. 1–12, 2024. [Online]. Available: <http://dx.doi.org/10.1109/TSE.2024.3407840>
- [12] J. Ayerdi, V. Terragni, A. Arrieta, P. Tonella, G. Sagardui, and M. Arratibel, "Generating metamorphic relations for cyber-physical systems with genetic programming: An industrial case study," in *Proceedings of the 29th ACM Joint Meeting on European Software Engineering Conference and Symposium on the Foundations of Software Engineering*, ser. ESEC/FSE 2021. New York, NY, USA: Association for Computing Machinery, 2021, p. 1264–1274. [Online]. Available: <https://doi.org/10.1145/3468264.3473920>
- [13] Y. Deng, X. Zheng, T. Zhang, H. Liu, G. Lou, M. Kim, and T. Y. Chen, "A declarative metamorphic testing framework for autonomous driving," *IEEE Transactions on Software Engineering*, pp. 1–20, 2022.
- [14] J. Ayerdi, A. Iriarte, P. Valle, I. Roman, M. Illarramendi, and A. Arrieta, "Marmot: Metamorphic runtime monitoring of autonomous driving systems," *ACM Trans. Softw. Eng. Methodol.*, jul 2024, just Accepted. [Online]. Available: <https://doi.org/10.1145/3678171>
- [15] R. Li, H. Liu, G. Lou, X. Zheng, X. Liu, and T. Y. Chen, "Metamorphic testing on multi-module uav systems," in *2021 36th IEEE/ACM International Conference on Automated Software Engineering (ASE)*, 2021, pp. 1171–1173.
- [16] K. Qiu, Z. Zheng, T. Y. Chen, and P.-L. Poon, "Theoretical and empirical analyses of the effectiveness of metamorphic relation composition," *IEEE Transactions on Software Engineering*, vol. 48, no. 3, pp. 1001–1017, 2022.
- [17] R. Matinnejad, S. Nejati, L. C. Briand, and T. Bruckmann, "Test generation and test prioritization for simulink models with dynamic behavior," *IEEE Transactions on Software Engineering*, vol. 45, no. 9, pp. 919–944, 2019.
- [18] M. Greiff, "Nonlinear control of unmanned aerial vehicles: Systems with an attitude," Doctoral Thesis (compilation), Department of Automatic Control, Oct. 2021.
- [19] C. Mandrioli, M. Nyberg Carlsson, and M. Maggio, "Testing abstractions for cyber-physical control systems," *ACM Trans. Softw. Eng. Methodol.*, vol. 33, no. 1, nov 2023. [Online]. Available: <https://doi.org/10.1145/3617170>
- [20] A. Arcuri and G. Fraser, "On parameter tuning in search based software engineering," in *Search Based Software Engineering*, M. B. Cohen and M. Ó Cinnéide, Eds. Berlin, Heidelberg: Springer Berlin Heidelberg, 2011, pp. 33–47.
- [21] C. Boufaied, M. Jukss, D. Bianculli, L. C. Briand, and Y. Isasi Parache, "Signal-based properties of cyber-physical systems: Taxonomy and logic-based characterization," *Journal of Systems and Software*, vol. 174, p. 110881, 2021. [Online]. Available: <https://www.sciencedirect.com/science/article/pii/S016421220302715>
- [22] J. Kapinski, X. Jin, J. V. Deshmukh, A. Donzé, T. Yamaguchi, H. Ito, T. Kaga, S. Kobuna, and S. A. Seshia, "St-lib: A library for specifying and classifying model behaviors," *SAE Technical Paper Series*, 2016.
- [23] C. A. Furia, D. Mandrioli, A. Morzenti, and M. Rossi, *Modeling Time in Computing*. Springer Publishing Company, Incorporated, 2012.
- [24] C. Menghi, E. Viganò, D. Bianculli, and L. C. Briand, "Trace-checking cps properties: Bridging the cyber-physical gap," in *Proceedings of the 43rd International Conference on Software Engineering*, ser. ICSE '21. IEEE Press, 2021, p. 847–859. [Online]. Available: <https://doi.org/10.1109/ICSE43902.2021.00082>
- [25] J. H. Dawes and D. Bianculli, "Specifying source code and signal-based behaviour of cyber-physical system components," in *Formal Aspects of Component Software*, S. L. Tapia Tarifa and J. Proença, Eds. Cham: Springer International Publishing, 2022, pp. 20–38.
- [26] C. Boufaied, C. Menghi, D. Bianculli, L. Briand, and Y. I. Parache, "Trace-checking signal-based temporal properties: A model-driven approach," in *Proceedings of the 35th IEEE/ACM International Conference on Automated Software Engineering*, ser. ASE '20. New York, NY, USA: Association for Computing Machinery, 2021, p. 1004–1015. [Online]. Available: <https://doi.org/10.1145/3324884.3416631>
- [27] J. Dawes and D. Bianculli, "Checking complex source code-level constraints using runtime verification," in *Companion Proceedings of the 32nd ACM International Conference on the Foundations of Software Engineering (FSE Companion '24)*. ACM, July 2024.

- [28] A. Kane, T. Fuhrman, and P. Koopman, "Monitor based oracles for cyber-physical system testing: Practical experience report," in *2014 44th Annual IEEE/IFIP International Conference on Dependable Systems and Networks*, 2014, pp. 148–155.
- [29] Z. He, Y. Chen, E. Huang, Q. Wang, Y. Pei, and H. Yuan, "A system identification based oracle for control-cps software fault localization," in *2019 IEEE/ACM 41st International Conference on Software Engineering (ICSE)*. United States of America: IEEE, 2019, pp. 116–127.
- [30] S. Bittanti, *Model Identification*. United States of America: John Wiley and Sons, Ltd, 2019, ch. 4, pp. 81–105. [Online]. Available: <https://onlinelibrary.wiley.com/doi/abs/10.1002/9781119546405.ch4>
- [31] L. V. Nguyen, J. Kapinski, X. Jin, J. V. Deshmukh, K. Butts, and T. T. Johnson, "Abnormal data classification using time-frequency temporal logic," in *Proceedings of the 20th International Conference on Hybrid Systems: Computation and Control*, ser. HSCC '17. New York, NY, USA: Association for Computing Machinery, 2017, p. 237–242. [Online]. Available: <https://doi.org/10.1145/3049797.3049809>
- [32] A. Donzé, O. Maler, E. Bartocci, D. Nickovic, R. Grosu, and S. Smolka, "On temporal logic and signal processing," in *Automated Technology for Verification and Analysis*, S. Chakraborty and M. Mukund, Eds. Berlin, Heidelberg: Springer Berlin Heidelberg, 2012, pp. 92–106.
- [33] C. Menghi, S. Nejati, L. Briand, and Y. I. Parache, "Approximation-refinement testing of compute-intensive cyber-physical models: an approach based on system identification," in *Proceedings of the ACM/IEEE 42nd International Conference on Software Engineering*, ser. ICSE '20. New York, NY, USA: Association for Computing Machinery, 2020, p. 372–384. [Online]. Available: <https://doi.org/10.1145/3377811.3380370>
- [34] A. Aleti and L. Grunske, "Test data generation with a kalman filter-based adaptive genetic algorithm," *Journal of Systems and Software*, vol. 103, pp. 343–352, 2015. [Online]. Available: <https://www.sciencedirect.com/science/article/pii/S0164121214002660>
- [35] T. Chen, F.-C. Kuo, W. Tam, and R. Merkel, "Testing a software-based pid controller using metamorphic testing," in *Proceedings of the 1st International Conference on Pervasive and Embedded Computing and Communication Systems*, C. Benavente-Peces and J. Filipe, Eds. Scitepress, 2011, pp. 387 – 396, international Conference on Pervasive and Embedded Computing and Communication Systems 2011, PECCS 2011 ; Conference date: 05-03-2011 Through 07-03-2011. [Online]. Available: <http://www.peccs.org/PECCS2011/>
- [36] J. Ayerdi, S. Segura, A. Arrieta, G. Sagardui, and M. Arratibel, "Qos-aware metamorphic testing: An elevation case study," in *2020 IEEE 31st International Symposium on Software Reliability Engineering (ISSRE)*, 2020, pp. 104–114.
- [37] J. Ayerdi, P. Valle, S. Segura, A. Arrieta, G. Sagardui, and M. Arratibel, "Performance-driven metamorphic testing of cyber-physical systems," *IEEE Transactions on Reliability*, pp. 1–19, 2022.